Preparation and Characterization of Nanofiber Nonwoven Textile for Electromagnetic Wave Shielding

Makoto Sonehara[1,2], Toshiro Sato[2], Midori Takasaki[1], Hajime Konishi[3], Kiyohito Yamasawa[2], and Yoshimasa Miura[2], *Fellow, IEEE*

[1]Satellite Venture Business Laboratory, Shinshu University, Ueda 386-8567, Japan
[2]Spin Device Technology Center, Shinshu University, Nagano 380-8553, Japan
[3]Faculty of Textile Science and Technology, Shinshu University, Ueda 386-8567, Japan

A nanofiber nonwoven textile with metallic magnetic material coating was fabricated, and the effect of electromagnetic wave shielding was evaluated. The nanofiber nonwoven textile with an average diameter of about 500 nm was spun by electrospinning. The metallic magnetic material was coated by sputtering on the textile surface. EMI shielding effect of the textile with metallic magnetic material coating was about 90% in the GHz band. Because the textile has thin, light, flexible, and breathable characteristics, it will be versatile for various electromagnetic wave shielding applications.

***Index Terms*—Electromagnetic wave shielding, electrospinning, metallic magnetic material, nanofiber nonwoven textile, sputtering.**

I. Introduction

Electromagnetic interference (EMI) has become extremely serious in various electronic equipment such as personal computers (a few GHz), cellular phones (0.8–2 GHz), electronic toll collection system (ETC, 5.8 GHz), broadcasting satellite (BS, 12 GHz) and others. EMI measures to prevent malfunctions of other electronic equipment are important. A noise suppressor filter and noise absorber sheet have been developed for EMI measures inside electronic equipment [1]–[3]. On the other hand, e.g., a magnetic wood has been studied for EMI measures outside electronic equipment [4].

This paper describes cloths with electromagnetic wave shielding effect. The cloths may apply, for example, for EMI measures at the medical equipment such as heart pacemakers. In this study, a nanofiber nonwoven textile with an average diameter of about 500 nm spun by electrospinning for electromagnetic wave shielding has been developed. A magnetic material was coated by a sputtering unit on the textile surface for reflecting and absorbing electromagnetic waves. Because the functional textile is light, flexible, and breathable, it will be versatile for various electromagnetic wave shielding applications.

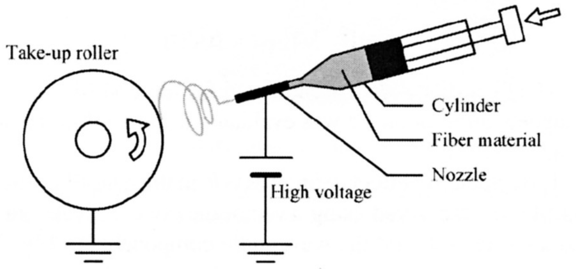

Fig. 1. Schematic of the electrospinning system.

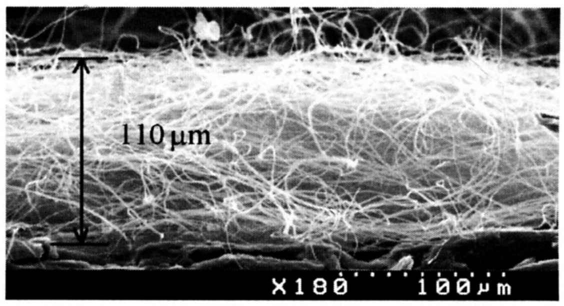

Fig. 2. SEM image of the cross section of the nanofiber nonwoven textile.

II. Fabrication

The raw material solution was made by stirring a mixture containing 12 wt.% of polyacrylonitrile (PAN) powder (Aldrich, mean molecular weight: 150000) and 88 wt.% of N,N-Dimethylformamide (DMF) (Wako pure chemical industries) at 70 °C for 6 h. The nanofiber nonwoven textile was prepared by electrospinning, as shown in Fig. 1 [5]. A high voltage of 12 kV was applied to the nozzle which is separated at a distance of 100 mm from the grounded take-up roller. The nanofiber nonwoven textile with a thickness of about 110 μm was obtained by electrospinning for 1 h. Fig. 2 shows an SEM image of the cross section of the nanofiber nonwoven textile.

Metallic magnetic material, $Ni_{83}Fe_{17}$ (at.%), was coated on the nanofiber nonwoven textile by RF magnetron sputtering at an Ar pressure of 0.5 Pa and RF power of 100 W. Ni-Fe with a low resistivity of about 25 $\mu\Omega \cdot$ cm was selected for a material of reflecting electromagnetic wave. In addition, Ni-Fe has ferromagnetic resonance effect for absorbing electromagnetic wave.

Ni-Fe of the same composition was sputter-coated on a continuous PAN film with a thickness of 30 μm (Mitsui Chemicals, Zexlon) for comparison with the nanofiber nonwoven textile.

Digital Object Identifier 10.1109/TMAG.2008.2002517

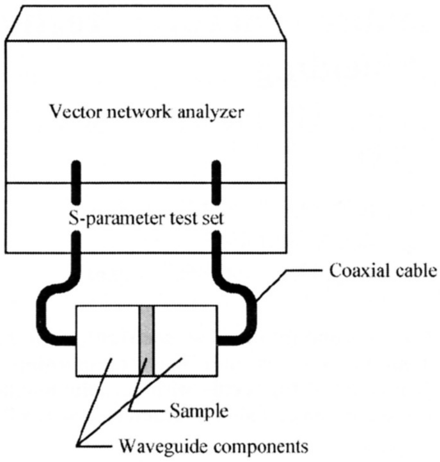

Fig. 3. Schematic of the measurement system.

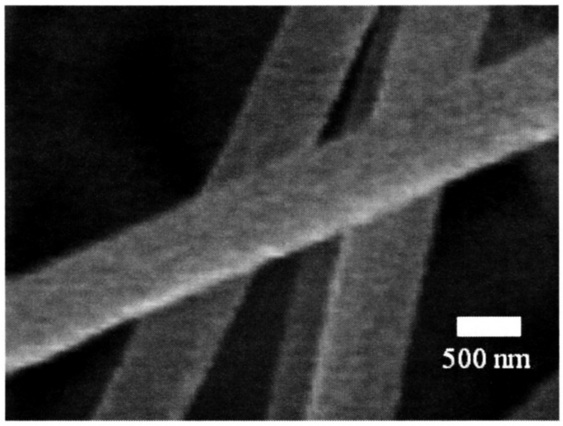

Fig. 4. SEM image of the nanofiber shielding textile with Ni-Fe coating with sputtering time t_s of 15 min.

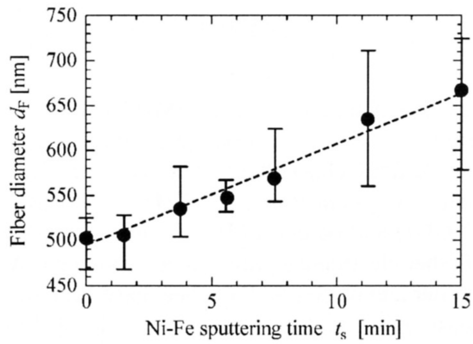

Fig. 5. Relation between the fiber diameter d_F and Ni-Fe sputtering time t_s in the nanofiber shielding textile with Ni-Fe coating.

III. Measurement

The fiber diameter was estimated from the SEM images. The magnetization of Ni-Fe was evaluated using a vibrating sample magnetometer.

EMI shielding effect defined as SE in the nanofiber shielding textile was measured using a vector network analyzer, an S-parameter test set, and the waveguide components in Fig. 3. The nanofiber shielding nonwoven textile sandwiched between the waveguide components was connected to the S-parameter test set.

SE was calculated with the following equations [6]:

$$SE = (P_{\text{ref}} + P_{\text{loss}})/P_{\text{in}} = 1 - 10^{(S_{21}[\text{dB}]/10)} \quad (1)$$

$$P_{\text{ref}}/P_{\text{in}} = 10^{(S_{11}[\text{dB}]/10)} \quad (2)$$

$$P_{\text{loss}}/P_{\text{in}} = 1 - \left(10^{(S_{11}[\text{dB}]/10)} + 10^{(S_{21}[\text{dB}]/10)}\right) \quad (3)$$

where P_{ref} is the reflective power, P_{loss} is the loss power, P_{in} is the input power, S_{11} is the input reflection coefficient, and S_{21} is the forward transmission coefficient. Both S_{11} and S_{21} for the nanofiber shielding textile were obtained by the vector network analyzer and the S-parameter test set.

IV. Results and Discussion

A. Relation Between Fiber Diameter and Ni-Fe Sputtering Time

Fig. 4 shows an SEM image of the nanofiber shielding nonwoven textile with Ni-Fe coating with a sputtering time t_s of 15 min. In Fig. 4, the fiber diameter with Ni-Fe coating was estimated to be about 660 nm, which was thicker than the fiber without Ni-Fe coating because of Ni-Fe thickness. The space between fibers was not filled with Ni-Fe, and the cloth kept the breathability. The magnetization of the fiber with Ni-Fe coating was one-ninth that of the PAN film with Ni-Fe coating. Most of Ni-Fe sputtered particles were passed through the gap between the fibers and reached the substrate holder, thus only a portion of Ni-Fe sputtered particles were deposited on the fibers.

Fig. 5 shows the relation between the fiber diameter d_F and Ni-Fe sputtering time t_s. Increase of the fiber diameter Δd_F is proportional to the sputtering time t_s.

B. EMI Shielding Effect

1) Frequency Dependence of EMI Shielding Effect and Sputtering Time of Ni-Fe: Fig. 6 shows the frequency dependences of $P_{\text{ref}}/P_{\text{in}}$, $P_{\text{loss}}/P_{\text{in}}$, $P_{\text{thru}}/P_{\text{in}}$, where $P_{\text{thru}}/P_{\text{in}}$ means $1 - (P_{\text{ref}} + P_{\text{loss}})/P_{\text{in}}$ in the nanofiber nonwoven textile (a) and the nanofiber shielding textile with Ni-Fe coating with a sputtering time t_s of 7.5 min (b) and 15 min (c). In Fig. 6(a), SE of the nanofiber shielding textile was about 10% in the measured frequency band. On the other hand, in Fig. 6(b), SE of the nanofiber nonwoven textile with Ni-Fe coating with a sputtering time t_s of 7.5 min was about 20% in the measured frequency band. In Fig. 6(c), SE of the textile with Ni-Fe coating with a sputtering time t_s of 15 min was about 90% in the measured frequency band. Increase of the Ni-Fe sputtering time t_s leads to the increase of $P_{\text{ref}}/P_{\text{in}}$ and $P_{\text{loss}}/P_{\text{in}}$, i.e., SE.

2) Relation Between EMI Shielding Effect and Sputtering Time of Magnetic Material: Fig. 7 shows the relation between $P_{\text{ref}}/P_{\text{in}}$, $P_{\text{loss}}/P_{\text{in}}$, $P_{\text{thru}}/P_{\text{in}}$, and Ni-Fe sputtering time t_s at

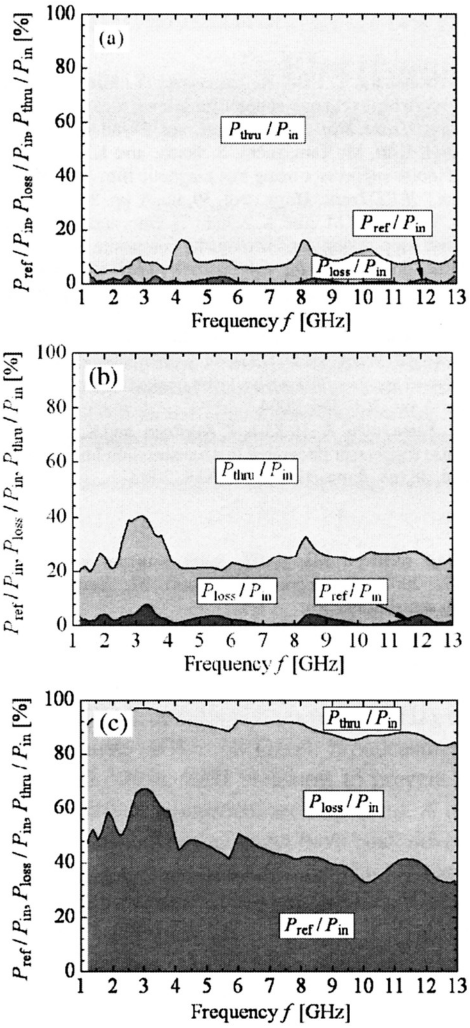

Fig. 6. Frequency dependences of P_{ref}/P_{in}, P_{loss}/P_{in}, and P_{thru}/P_{in} in (a) the nanofiber nonwoven textile and the nanofiber shielding textile with Ni-Fe coating with a sputtering time t_s of (b) 7.5 min and (c) 15 min.

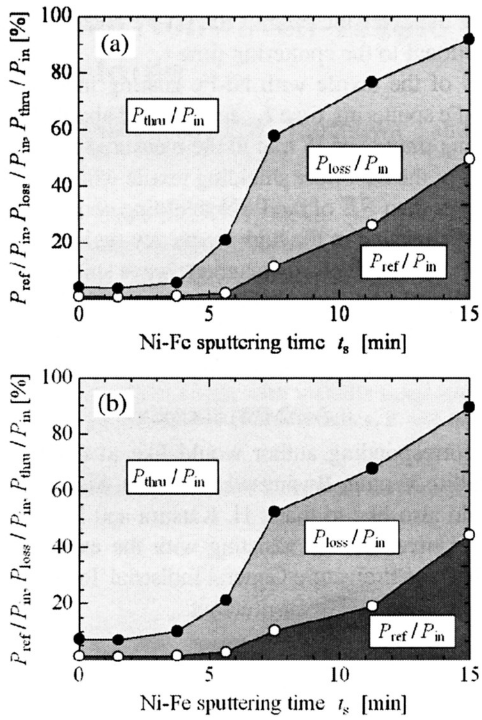

Fig. 7. Relation between P_{ref}/P_{in}, P_{loss}/P_{in}, P_{thru}/P_{in}, and Ni-Fe sputtering time t_s at (a) 1.6 GHz and (b) 5.8 GHz in the nanofiber shielding textile with Ni-Fe coating.

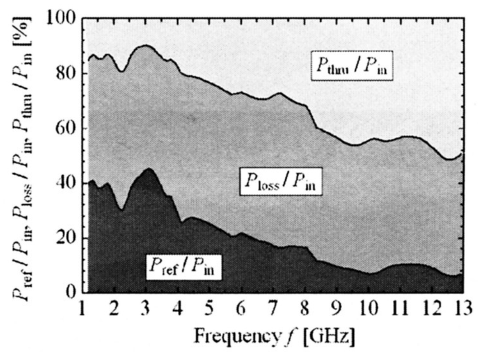

Fig. 8. Frequency dependence of P_{ref}/P_{in}, P_{loss}/P_{in}, and P_{thru}/P_{in} in the PAN shielding film with Ni-Fe coating with a sputtering time t_s of 1.7 min.

1.6 GHz (i.e., second-harmonic frequency of 0.8 GHz for cellular phones) (a) and 5.8 GHz (i.e., fundamental frequency for ETC) (b). The trend in Fig. 7(a) and (b) are very similar, i.e., when increasing the Ni-Fe sputtering time t_s, both P_{ref}/P_{in} and P_{loss}/P_{in} increased in both figures. The nanofiber shielding textile with Ni-Fe coating showed sufficient reflection and absorbance of the electromagnetic wave.

C. Comparison of the Nanofiber Shielding Textile With Ni-Fe Coating and the PAN Shielding Film With Ni-Fe Coating

Fig. 8 shows the frequency dependence of P_{ref}/P_{in}, P_{loss}/P_{in}, and P_{thru}/P_{in} in the PAN shielding film with Ni-Fe coating sputtering time t_s of 1.7 min. The volume of Ni-Fe coating on the PAN film in Fig. 8 was adjusted to correspond to the volume of Ni-Fe coating in the nanofiber shielding nonwoven textile with Ni-Fe coating with sputtering time t_s of 15 min in Fig. 6(c).

In Fig. 8, SE of the PAN shielding film with Ni-Fe coating with a sputtering time t_s of 1.7 min was about 90% at 1 GHz. The result is approximately consistent with the result of the textile with Ni-Fe coating in Fig. 6(c). Although P_{loss}/P_{in} was constant, P_{ref}/P_{in} decreased, leading to a decrease in SE when the Ni-Fe coating was not sufficiently thick to reflect the electromagnetic wave in the high frequency. On the other hand, the nanofiber shielding nonwoven textile has a hierarchical structure of the fiber matrix, and fibers not only at the surface of the textile but also inside the textile are coated with Ni-Fe. The electromagnetic wave passes through the surface fibers, the through electromagnetic wave is reflected by the fibers at each depth through the textile, and high SE is obtained even in the high-frequency region.

V. Conclusion

The nanofiber shielding nonwoven textile with Ni-Fe coating was investigated. The results obtained are as follows.

1) The diameter increase of the Ni-Fe coated fiber was proportional to the sputtering time t_s.
2) SE of the textile with Ni-Fe coating increased with the Ni-Fe sputtering time t_s, and reached about 90% at a sputtering time t_s of 15 min in the measured frequency band.
3) SE of the nanofiber shielding textile with Ni-Fe coating is higher than SE of the PAN shielding continuous film with Ni-Fe coating in the high frequency region.

The textile has an electromagnetic wave shielding ability that is light, flexible, and breathable. The materials for various electromagnetic wave shielding applications are expected with this nanofiber shielding nonwoven textile.

ACKNOWLEDGMENT

The corresponding author would like to thank the staff of the Satellite Venture Business Laboratory, Shinshu University. He would also like to thank H. Katsura and Prof. T. Koyama, Shinshu University, for assisting with the experiment and K. Kudo, Nagano Prefecture General Indistrial Technology Center, for assisting with the measurement.

REFERENCES

[1] M. Sonehara, T. Sato, K. Yamasawa, Y. Miura, and M. Yamaguchi, "FeSi/IrMn exchange-coupled multilayer film with plural FMR absorptions," *Trans. Mat. Res. Soc. Jpn.*, vol. 29, no. 4, pp. 1735–1738, 2004.

[2] K.-H. Kim, M. Yamaguchi, S. Ikeda, and K.-I. Arai, "Modeling for RF noise suppressor using soft magnetic film on coplanar transmission line," *IEEE Trans. Magn.*, vol. 39, no. 5, pp. 3031–3033, Oct. 2003.

[3] N. Matsushita, M. Abe, K. Kondo, H. Ono, and S. Yoshida, "Conducted noise suppression in GHz range by composite sheets and ferrite-plated films," in *Proc. 9th Int. Conf. Ferrites (ICF-9)*, 2004, pp. 739–746.

[4] H. Oka, K. Narita, H. Osada, and K. Seki, "Experimental results on indoor electromagnetic wave absorber using magnetic wood," *J. Appl. Phys.*, vol. 91, no. 10, pp. 7008–7010, 2002.

[5] D. Li, Y. Wang, and Y. Xia, "Electrospinning nanofibers as uniaxial aligned arrays and layer-by-layer stacked films," *Adv. Mater.*, vol. 16, no. 4, pp. 361–366, 2004.

[6] M. Yamaguchi, K.-H. Kim, T. Kuribara, and K.-I. Arai, "Thin film RF noise suppressor integrated in a transmission line," *IEEE Trans. Magn.*, vol. 38, no. 5, pp. 3183–3185, Oct. 2002.

Manuscript received March 03, 2008. Current version published December 17, 2008. Corresponding author: M. Sonehara (e-mail: sonehara@yslab.shinshu-u.ac.jp).